# Fuel-Optimal Cruising Strategy for Road Vehicles With Step-Gear Mechanical Transmission

**Article** *in* IEEE Transactions on Intelligent Transportation Systems · August 2015

DOI: 10.1109/TITS.2015.2459722

CITATIONS
34

READS
397

**5 authors**, including:

Shaobing Xu
Tsinghua University
**13** PUBLICATIONS **219** CITATIONS
SEE PROFILE

Shengbo Eben Li
Tsinghua University
**191** PUBLICATIONS **4,875** CITATIONS
SEE PROFILE

Xiaowu Zhang
Ford Motor Company, Dearborn, Michigan, United States
**25** PUBLICATIONS **680** CITATIONS
SEE PROFILE

Huei Peng
University of Michigan
**342** PUBLICATIONS **16,526** CITATIONS
SEE PROFILE

# Fuel-Optimal Cruising Strategy for Road Vehicles With Step-Gear Mechanical Transmission

Shaobing Xu, Shengbo Eben Li, *Member, IEEE*, Xiaowu Zhang, Bo Cheng, and Huei Peng

***Abstract*—This paper studies the principles and mechanism of a fuel-optimal strategy in cruising scenarios, i.e., the pulse and glide (PnG) operation, for road vehicles equipped with a step-gear transmission. In the PnG strategy, the control of the engine and the transmission determines the fuel-saving performance, and it is obtained by solving an optimal control problem (OCP). Due to a discrete gear ratio, strong nonlinear engine fuel characteristics, and different dynamics in the pulse/glide mode, the OCP is a switching nonlinear mixed-integer problem. This challenging problem is converted by a knotting technique and the Legendre pseudospectral method to a nonlinear programming problem, which then solves the optimal engine torque and transmission gear position. The optimization results show the significant fuel saving of the PnG operation as compared with the constant-speed cruising strategy. The underlying fuel-saving mechanism of the PnG strategy is explained graphically. For a real-time implementation, a near-optimal practical rule that enables a driver and/or an automatic control system to fast select gear positions and engine torque profile is proposed with only slightly deteriorated fuel saving.**

***Index Terms*—Eco-driving, cruising strategy, pulse and glide, optimal control, pseudo-spectral method.**

## I. Introduction

IMPROVING fuel economy of road vehicles is gaining interest, driven by the concerns on environmental protection, energy security, and customer demand [1], [2]. Fuel saving techniques such as hybrids, clean combustion, and lightweight have been developed continuously [1]. However, the fuel economy of road vehicles not only depends on the characteristics of the powertrain components, but also depends on how a vehicle is driven [1], [3]. It was shown that different driving operations can lead to 10%–15% fuel consumption difference under identical conditions [1], [4]. Boriboonsomsin *et al.* (2011) showed that the best fuel improvement can be 24% by providing qualitative advices to drivers, e.g., shift gear sooner and accelerate softly, to change the driving behaviors [5]. Malikopoulos *et al.* constructed an eco-driving optimization framework that achieved about 20% fuel savings, and then designed a real-time feedback system with visual instructions to alter driving behavior [6]. Riener designed a subliminal persuasion method that applied tactile feedback by vibratable safety belt and car seat to inspire economical driving behavior, and observed about 8% fuel consumption improvement in real-car tests [7]. A practical eco-driving app aimed at improving driving efficiency by providing operation recommendations was also presented in [8]. These results indicate the fuel saving potential of economical driving, which can be implemented by education, driver assistance systems, and automated driving. Whatever the embodiment, a firm understanding of the fuel saving strategy is required. For education, the qualitative driving tips like "accelerate softly" are acceptable, while for automatic control system, quantitative strategies are needed.

Cruising, as the most common maneuver, consumes a significant portion of the total energy consumption, e.g., 35% in urban conditions [9], and higher in highway driving. A survey showed that coach buses spend 65–78% of total driving time cruising on the freeway in Beijing [10]. Therefore, fuel-saving cruising techniques can have significant effect, 1% fuel saving in cruising scenarios can reduce about 20 million barrels of oil per year in the world [11]. The commonly used cruising strategy is the constant speed (CS) operation, i.e., traveling at a fixed speed, which is frequently adopted by drivers and cruising control systems. However, due to the strong nonlinearity of engine efficiency, CS is not always the fuel optimal strategy. Pulse and Glide (PnG) type cruising strategy, also called accelerating and coasting strategy, has been proven to achieve better fuel economy by theoretical calculations and experiments, and the fuel saving rate can be up to 20% [12], [13].

PnG strategy is a dynamic cruising strategy: drivers or control systems need to accelerate the vehicle from a low speed to a higher speed first, called the pulse (or accelerating) phase, and then coast to the lower speed, called the glide (or coasting) phase [13], with the average speed equal to the expected velocity. Compared to CS, PnG requires periodical fluctuations on vehicle speed and dynamic controls on engine and transmission. Although this strategy has great potential to reduce fuel consumption, not all accelerating operations can achieve the goal of fuel saving [12]. The dynamic control inputs, i.e., engine

Manuscript received February 12, 2015; revised May 19, 2015; accepted July 19, 2015. Date of publication August 19, 2015; date of current version November 23, 2015. This work was supported in part by the National Science Foundation of China under Grant 51205228 and in part by Tsinghua University Initiative Scientific Research Program under Grant 2012THZ0. The Associate Editor for this paper was P. Zingaretti.

S. Xu and S. E. Li are with State Key Laboratory of Automotive Safety and Energy, Department of Automotive Engineering, School of Mechanical Engineering, Tsinghua University, Beijing 100084, China (e-mail: xsbing2008@foxmail.com; lisb04@gmail.com).

X. Zhang is with the Department of Mechanical Engineering, College of Engineering, University of Michigan, Ann Arbor, MI 48109 USA (e-mail: xiaowuz@umich.edu).

B. Cheng is with State Key Laboratory of Automotive Safety and Energy, Department of Automotive Engineering, Suzhou Automotive Research Institute, Tsinghua University, Beijing 100084, China (e-mail: chengbo@tsinghua.edu.cn).

H. Peng is with the Department of Mechanical Engineering, College of Engineering, University of Michigan, Ann Arbor, MI 48109 USA, and also with State Key Laboratory of Automotive Safety and Energy, Department of Automotive Engineering, School of Mechanical Engineering, Tsinghua University, Beijing 100084, China (e-mail: hpeng@umich.edu).

Color versions of one or more of the figures in this paper are available online at http://ieeexplore.ieee.org.

Digital Object Identifier 10.1109/TITS.2015.2459722

output torque and gear position, should be carefully selected. Improper control inputs, e.g., following the qualitative tips like "accelerate softly", may even cause more fuel consumption than CS [13].

For vehicles with continuously variable transmission (CVT), Li and Peng optimized the PnG strategy under an optimal control framework [13], [15]. For the particular vehicle/engine they studied, it was found that depending on the vehicle speed, the best strategy can vary from PnG to CS [13], [14]. The speed-dependent behavior arises from the nonlinear characteristics of the internal combustion engine [13]. The fuel saved by such periodic control can be as high as 20% [14]. Lee and Nelson further validated the fuel saving potential of PnG through large scale real car experiments [12].

For vehicles with step-gear transmission, the related optimal control problem is more difficult because of the discrete gear ratios. For the CVT-type vehicles, thanks to the continuous gear ratio, the engine can be forced to operate on the best efficiency line by continuously changing gear ratio, then the engine power becomes the only control input and the switching problem is approximated by a continuous problem [13]–[15]. However, if the gear ratio is discrete, the optimal control problem cannot be approximated as a continuous one, and the dynamics in the accelerating mode and the coasting mode are completely different, thus the problem is a switching nonlinear mixed-integer problem, which is challenging to solve [16], [17]. One of the existing feasible approaches is to convert it into mixed-integer programming, which then could be solved by methods such as branch & bound and cutting planes [18], [19]. In addition, the fuel saving mechanism of PnG strategy for vehicles with discrete gears is unclear and should be carefully studied; since the nonlinear optimization is often time consuming and not suitable for online implementation, a computationally inexpensive control rule is also needed to real-time execute PnG strategy.

The contributions of this paper are to (1) obtain the fuel-optimal cruising strategy (control of engine and transmission) for road vehicles with step-gear transmission, (2) present the underlying fuel saving mechanism of the optimal strategy, and (3) for real-time implementation, propose a near-optimal practical rule that enables driver and automatic control system to fast determine gear positions and engine torque profile as compared with the original nonlinear optimization solution. The optimization of PnG-type strategy is converted into a nonlinear optimal control problem (OCP) with discrete control inputs and discontinuous switching between the accelerating mode and the coasting mode. To handle the discontinuity, a multi-phase knotting technology combining Legendre pseudospectral discretization is adopted to convert the OCP into a high-dimensional sparse nonlinear programming problem. The fuel saving capacity, mechanism of the PnG strategy and practical control rule are then presented.

The rest of the paper is organized as follows: Section II formulates the fuel-optimal cruising problem; Section III presents the method of converting OCP into nonlinear programming problem for numerical computations; Section IV shows the optimization results; Section V explains the mechanism of the PnG strategy; Section VI presents a practical control rule of engine and transmission, and Section VII concludes this paper.

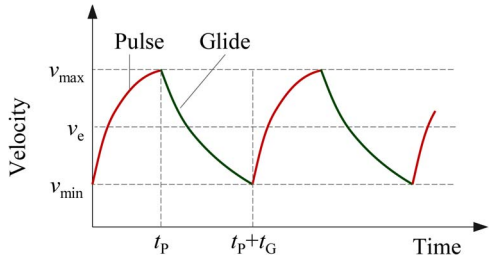


Fig. 1. Concept of the PnG strategy.

## II. Fuel-Optimal Cruising Problem

The PnG strategy is shown in Fig. 1. When the expected cruising speed is $v_e$, the vehicle first accelerates from a low speed $v_{\min}$ to a higher speed $v_{\max}$ in the "accelerating phase" and then coast down to $v_{\min}$ in the "coasting phase," with the average speed equal to the desired velocity $v_e$. This strategy can be used in situations with sparse traffic, e.g., driving on low-density highways and suburban roads. Our goal is to determine the optimal gear position and engine torque profile to minimize the fuel consumption.

This problem naturally fits into the optimal control framework with engine torque and gear position as the control variables. The performance index, state space equations, and constraints of this fuel-optimal control problem are described in the following.

In the PnG strategy, the coasting rules significantly affect the fuel saving performance, which are often ignored. Though coasting with engine idling and transmission in neutral is often selected by default [12], [13], here we study four types of coasting strategies:

(a) PnG-N-O, coasting with transmission in neutral and engine shut off;
(b) PnG-N-I, coasting with transmission in neutral and engine idling;
(c) PnG-G-D, coasting with transmission in gear, and the gears for accelerating and coasting can be different;
(d) PnG-G-S, coasting with transmission in gear and the gears for accelerating and coasting are same, which can avoid frequent gear shifting.

The models of these four PnG strategies are different but similar, so we only present the model of PnG-G-S in details, and the others are only introduced briefly. Since the speed fluctuations of PnG is generally small, to avoid excessive complexity, we assume that only a particular gear is used to accelerate and to coast, i.e., gear shifting only happens at the beginning of accelerating or coasting.

### A. Performance Index to Assess Fuel Economy

The index "fuel consumption per 100 kilometers" is adopted to measure the fuel economy of different cruising strategies, defined as

$$J = \frac{\int_0^{t_P} \mathcal{F}_P \mathrm{d}t + \int_{t_P}^{t_P+t_G} \mathcal{F}_G \mathrm{d}t}{s_P + s_G} \tag{1}$$

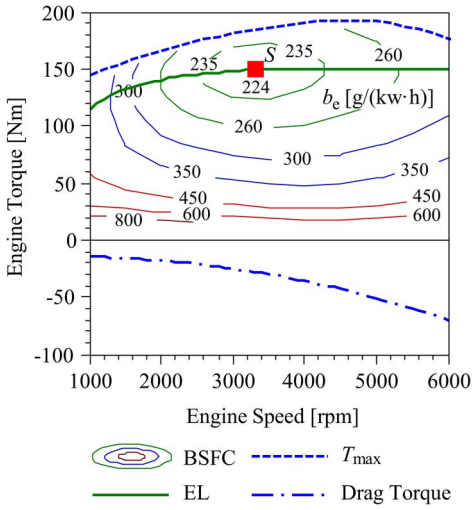


Fig. 2. Engine model.

where, $t_P$, $\mathcal{F}_P$, and $s_P$ ($t_G$, $\mathcal{F}_G$, and $s_G$) denote the duration, engine fuel injection rate, and terminal distance of the pulse phase (glide phase), respectively.

In the pulse phase, the analytical function for the engine fuel injection rate $\mathcal{F}_P$ is derived from engine test data. It is fitted by a 2-dimensional 4th-order polynomial:

$$\mathcal{F}_P(T_\mathrm{e}, w_\mathrm{e}) = \sum_{i=0}^{4}\sum_{j=0}^{i} k_{\mathcal{F},1+j+\sum_0^i n} T_\mathrm{e}^{i-j} w_\mathrm{e}^{j} \tag{2}$$

where $k_{\mathcal{F},\#}$ are the fitting coefficients. The relationship $\mathcal{F}_P = b_\mathrm{e} \cdot P_\mathrm{e}$ gives the engine brake specific fuel consumption (BSFC) $b_\mathrm{e}$, where $P_\mathrm{e}$ is the engine power. The BSFC is plotted in Fig. 2. The maximum engine torque $T_\mathrm{max}$ is fitted similarly by a 1-dimensional 4th-order polynomial:

$$T_\mathrm{max}(w_\mathrm{e}) = \sum_{i=0}^{4} k_{\mathrm{max},i} w_\mathrm{e}^{i} \tag{3}$$

where $k_{\mathrm{max},i}$ are the fitting coefficients. The fitting result of $T_\mathrm{max}$ is shown in Fig. 2 as the dashed line.

In reality, a steady-state engine map does not accurately predict the fuel consumption of dynamic driving process. The transient dynamics of engine can cause reduction in volumetric efficiency and transient wall wetting, thus reducing actual output torque compared to the statically calibrated engine test data. A correction term related to the derivative of engine speed is used [20]:

$$T_\mathrm{ed} = T_\mathrm{e}\left(1 - \gamma_\mathrm{d}\frac{\mathrm{d}w_\mathrm{e}}{\mathrm{d}t}\right) \tag{4}$$

where, $\gamma_\mathrm{d}$ is the dynamic correction coefficient, and $T_\mathrm{ed}$ represents the dynamic engine torque. In addition, one critical curve related to the engine efficiency is introduced here, i.e., EL, as shown in Fig. 2, represents the collection of most efficient points under a given engine speed. The highest-efficiency point of BSFC will be called the "sweet spot" in the following sections, i.e., point S in Fig. 2.

In the glide phase of PnG-G-S, the vehicle coasts with the transmission in gear. Due to the electronically controlled fuel injection technology, the engine can automatically cut off fuel supply when coasting with the accelerator pedal fully released and engine speed higher than a threshold (1000 rpm here). This function is called deceleration fuel cut off [21]. Assuming these conditions are met, the fuel injection rate $\mathcal{F}_G$ is zero, i.e.,

$$\mathcal{F}_G = 0. \tag{5}$$

### B. Vehicle Longitudinal Model for Control

The studied vehicle powertrain includes an engine, a clutch, and an automated manual transmission (AMT) with discrete gear ratios. Considering both simplicity and accuracy, three assumptions are made: i) the high-order dynamics of rotating parts in engine and transmission, as well as torsional deformation of entire driveline are not considered; ii) the gear shifting is executed instantaneously, the disengagement and slip of clutch are neglected; iii) the transmission efficiency under different gear ratios and different power is assumed to be the same.

In the pulse phase, the engine drives the vehicle to accelerate from an initial velocity $v_{0,P}$ to a higher terminal velocity $v_{f,P}$. The distance $s$, velocity $v$ and acceleration $a$ satisfy:

$$\begin{aligned} \dot{s} &= v \\ \dot{v} &= a. \end{aligned} \tag{6}$$

From the force balance equation, one gets:

$$\frac{i_0\eta_T}{r_w} i_\mathrm{g} T_\mathrm{ed} = \delta_{i_\mathrm{g}} M\dot{v} + k_a v^2 + k_f \tag{7}$$

where, $i_\mathrm{g}$ and $i_0$ are the gear ratio of the transmission and final gear, respectively; $r_w$ is the tire effective radius; $\eta_\mathrm{T}$ is the total efficiency of the driveline; $\delta_{i_\mathrm{g}}$ denotes the rotational inertial coefficient; $k_a = 0.5 C_\mathrm{D}\rho_\mathrm{a}A_v$, and $k_f = Mgf$ are related to the aerodynamic drag force and rolling resistance, $C_\mathrm{D}$ is the aerodynamic drag coefficient, $\rho_\mathrm{a}$ is the air density, $A_v$ is the frontal area of the vehicle, $f$ is the rolling resistance coefficient, $M$ and $g$ represent the vehicle mass and the gravity constant.

The relationship between the engine speed $w_\mathrm{e}$ (rpm) and vehicle speed $v$ is

$$w_\mathrm{e} = k_w v i_\mathrm{g},\ k_w = \frac{30}{\pi r_w} \tag{8}$$

where $k_w$ is a simplified coefficient.

Considering the gear ratio is fixed in the pulse phase, Eq. (4) is simplified to

$$T_\mathrm{ed} = T_\mathrm{e}(1 - \gamma_\mathrm{d} k_w i_\mathrm{g}\dot{v}). \tag{9}$$

Substituting (7) and (9) into (6), we have the longitudinal motion equation of the pulse phase expressed as:

$$\begin{aligned} \dot{s} &= v \\ \dot{v} &= \frac{i_\mathrm{g} i_0 \eta_T T_\mathrm{e}/r_w - k_a v^2 - k_f}{\delta_{i_\mathrm{g}} M + i_0\eta_T\gamma_\mathrm{d}k_w i_\mathrm{g}^2 T_\mathrm{e}/r_w}. \end{aligned} \tag{10}$$

TABLE I
KEY PARAMETERS OF THE VEHICLE DYNAMICS

| Parameters | Value | Parameters | Value |
|---|---|---|---|
| $\gamma_{\mathrm{d}}$ | 0.003 s$^2$/rad | $C_{\mathrm{D}}$ | 0.316 |
| $\mathcal{F}_I$ | 0.1535 g/s | $A_v$ | 2.22 m$^2$ |
| $i_0$ | 3.863 | $M$ | 1600 kg |
| $\eta_{\mathrm{T}}$ | 0.9 | $f$ | 0.028 |
| $r_w$ | 0.307 m | $w_{\min}$ | 1000 rpm |
| $\rho_{\mathrm{a}}$ | 1.226 kg/m$^3$ | $w_{\max}$ | 6000 rpm |
| $\alpha_0, \alpha_1, \alpha_2$ | -16, 19.5,-84.5 | | |
| $i_{\mathrm{g}}$ | 3.620, 1.925, 1.285, 0.933, 0.692 | | |
| $\delta_{i_{\mathrm{g}}}$ | 1.322, 1.112, 1.067, 1.049, 1.041 | | |

In the glide phase, the vehicle coasts from an initial velocity $v_{0,G}$ to a lower terminal velocity $v_{f,G}$ by dissipating the stored kinetic energy. The coasting resistance consists of two parts, (i) rolling resistance and aerodynamic drag force; (ii) the engine drag torque arising from "frictional and air-pumping," exists when coasting with transmission in gear. So the equations for coasting in gear are

$$\begin{aligned} \dot{s} &= v \\ \dot{v} &= \frac{i_0 i_{\mathrm{g}}}{\delta_{i_{\mathrm{g}}} M r_w} \frac{T_{\mathrm{er}}(w_{\mathrm{e}})}{\eta_{\mathrm{T}}} - \frac{k_a v^2 + k_f}{\delta_{i_{\mathrm{g}}} M} \end{aligned} \tag{11}$$

where $T_{\mathrm{er}}$ is the engine drag torque, which is shown in Fig. 2 as the dash-dot line, fitted as

$$T_{\mathrm{er}}(w_{\mathrm{e}}) = \alpha_0 + \alpha_1 \left(\frac{w_{\mathrm{e}}}{6500}\right) + \alpha_2 \left(\frac{w_{\mathrm{e}}}{6500}\right)^2 \tag{12}$$

where $\alpha_0$, $\alpha_1$, and $\alpha_2$ are the fitting coefficients.

### C. Constraints From the Cruising Operation

The constraints arise from the physical limits of powertrain and the features of PnG. The first one involves the engine speed, engine torque, and gear ratio, i.e.,

$$\begin{aligned} w_{\mathrm{emin}} \le w_{\mathrm{e}} \le w_{\mathrm{emax}} \\ 0 < T_{\mathrm{e}} \le T_{\max}(w_{\mathrm{e}}) \\ i_{\mathrm{g}} \in \{i_{\mathrm{g1}}, i_{\mathrm{g2}}, i_{\mathrm{g3}}, i_{\mathrm{g4}}, i_{\mathrm{g5}}\}. \end{aligned} \tag{13}$$

The second one consists of two parts, (i) the average velocity $\bar{v}$ constraint:

$$\bar{v} = \frac{s_P + s_G}{t_P + t_G} = v_{\mathrm{e}}. \tag{14}$$

(ii) The initial velocity $v_{0,P}$ (terminal velocity $v_{f,P}$) of the pulse phase is equal to the terminal velocity $v_{f,G}$ (initial velocity $v_{0,G}$) of glide phase, i.e.,

$$\begin{aligned} v_{0,P} = v_{f,G} = (1-\beta)\bar{v} \\ v_{f,P} = v_{0,G} = (1+\beta)\bar{v} \end{aligned} \tag{15}$$

where $\beta$ is a given coefficient of velocity fluctuation.

Besides the engine model introduced in Section II-A, the other parameters are listed in Table I.

### D. Optimal Control Problem

The resulting fuel optimal control problem of PnG-G-S is stated as following:

$$\min\ J = \frac{\int_0^{t_P} F_P \mathrm{d}t + \int_{t_P}^{t_P+t_G} F_G \mathrm{d}t}{s_P + s_G}$$

Subject to

$$\begin{aligned} \dot{s} &= v \\ \dot{v} &= \begin{cases} \dfrac{i_{\mathrm{g}} i_0 \eta_T T_{\mathrm{e}}/r_w - k_a v^2 - k_f}{\delta_{i_{\mathrm{g}}} M + i_0 \eta_T \gamma_{\mathrm{d}} k_w i_{\mathrm{g}}^2 T_{\mathrm{e}}/r_w} & \text{In the pulse phase} \\ \dfrac{i_0 i_{\mathrm{g}}}{\delta_{i_{\mathrm{g}}} M r_w} \dfrac{T_{\mathrm{er}}}{\eta_{\mathrm{T}}} - \dfrac{k_a v^2 + k_f}{\delta_{i_{\mathrm{g}}} M} & \text{In the glide phase} \end{cases} \\ T_{\mathrm{er}} &= \alpha_0 + \alpha_1 \left(\frac{w_{\mathrm{e}}}{6500}\right) + \alpha_2 \left(\frac{w_{\mathrm{e}}}{6500}\right)^2 \\ w_{\mathrm{e}} &= k_w v i_{\mathrm{g}} \\ \bar{v} &= v_{\mathrm{e}} \\ v_{0,P} = v_{f,G} &= (1-\beta)\bar{v} \\ v_{f,P} = v_{0,G} &= (1+\beta)\bar{v} \\ w_{\mathrm{emin}} \le w_{\mathrm{e}} &\le w_{\mathrm{emax}} \\ 0 < T_{\mathrm{e}} &\le T_{\max}(w_{\mathrm{e}}) \\ i_{\mathrm{g}} &\in \{i_{\mathrm{g1}}, i_{\mathrm{g2}}, i_{\mathrm{g3}}, i_{\mathrm{g4}}, i_{\mathrm{g5}}\}. \end{aligned} \tag{16}$$

The states are the distance $s$ and velocity $v$, denoted as $\boldsymbol{x} = (s, v)^{\mathrm{T}}$, and control inputs are the engine torque $T_{\mathrm{e}}$, engine drag torque $T_{\mathrm{er}}$ and gear ratio $i_{\mathrm{g}}$. The models of PnG-N-O, PnG-N-I, and PnG-G-D can be taken as a special case of the model of PnG-G-S, i.e.,

(a) For the model of PnG-N-O, setting $\mathcal{F}_G = 0$ and $T_{\mathrm{er}} = 0$.
(b) For the model of PnG-N-I, setting $\mathcal{F}_G = \mathcal{F}_I$ and $T_{\mathrm{er}} = 0$, where $\mathcal{F}_I$ is the idling fuel injection rate.
(c) Taking the gear ratios in the accelerating phase and the coasting phase as independent variables results in the model of PnG-G-D.

The aforementioned OCP (16) has two known modes/phases (i.e., pulse first and then glide), discrete control input (i.e., the gear ratio of transmission), and strong nonlinear engine fuel characteristics, it is thus a switching nonlinear mixed-integer problem. This paper will employ the multi-phase knotting pseudospectral method to convert the non-smooth OCP into a nonlinear programming (NLP) problem for more accurate numerical computation.

## III. OPTIMIZATION USING MULTI-PHASE KNOTTING PSEUDOSPECTRAL METHOD

The multi-phase knotting pseudospectral method, an extension of the pseudospectral method (PM), is an effective technique to address non-smoothing OCP [22]. The pseudospectral method is an effective global collocation method to convert a smooth OCP into an NLP [23]–[26]. The fundamental is to discretize the OCP at orthogonal collocation points, then employ global rather than local interpolation polynomials to

approximate states and control inputs, which ensures the high accuracy, and thus convert OCP into associated NLP. Compared to the conventional methods, e.g., shooting method, PM has better accuracy and convergence speed [23]. There are three classic types of PM in the literatures: Gauss, Radau, and Legendre. Compared to the other two types, the Legendre PM has better convergence for OCP with initial and terminal state constraints and is better at handling boundary constraints [25]. Therefore, we choose the Legendre PM to solve the problem (16).

It should be noted that pseudospectral methods are not able to directly handle non-smooth OCP because of the low accuracy when using finite-order interpolation polynomials to approximate infinite-order non-smooth curves. To overcome the discontinuity of this fuel-optimal cruising problem, we adopt the knotting technique to convert the non-smooth OCP into two smooth sub-stages, corresponding to accelerating and coasting phases. The speed and distance at the switching point are constrained to be equal. The optimal solutions are then obtained by the collaborative optimization of the two sub-stages. To simplify the expression, we record the initial time as $T_0$, and record the terminal time $t_P$ of the pulse phase and the terminal time $(t_P + t_G)$ of the PnG as $T_1$ and $T_2$. The process of converting the OCP is described below:

*1) Conversion of Time Interval:* Each time interval of the two stages is transformed into a canonical interval $[-1,1]$ by

$$\tau = \frac{2t - (T_q + T_{q-1})}{T_q - T_{q-1}} \tag{17}$$

where $q = 1, 2$.

*2) Collocation Points and Approximation:* The Legendre PM uses the Legendre-Gauss-Lobatto points, which are the roots of the derivative of $N$th order Legendre polynomial, together with two end points $-1$ and 1. Each phase can set different number of collocation points, denoted as $N_q + 1$. The points at the $q$th phase are denoted as $\tau_{q,i}$, where $i = 0, 1, \ldots, N_q$. The states $s$ and $v$ are discretized to be

$$\boldsymbol{X}_q = \begin{bmatrix} \mathbb{S}_{q,0} & \mathbb{S}_{q,1} & \cdots & \mathbb{S}_{q,N_q} \\ \mathbb{V}_{q,0} & \mathbb{V}_{q,1} & \cdots & \mathbb{V}_{q,N_q} \end{bmatrix}. \tag{18}$$

The engine torque $T_\mathrm{e}$ in the pulse phase is discretized to $\mathbb{T}_{1,i}$, and the engine drag torque $T_\mathrm{er}$ in the glide phase is discretized to $\mathbb{T}_{2,i}$, where $i = 0, 1, \ldots, N_q$. Note that we only optimize the discretized points $\boldsymbol{X}_{q,i}$ and $\mathbb{T}_{q,i}$, the dynamic $\boldsymbol{x}_q(\tau)$ and $T_\mathrm{e}(\tau)$ are obtained by Lagrange interpolation at the collocation points, i.e.,

$$\begin{aligned} \boldsymbol{x}_q(\tau) &\approx \sum_{i=0}^{N_q} L_{q,i}(\tau) \boldsymbol{X}_{q,i} \\ T_\mathrm{e}(\tau) &\approx \sum_{i=0}^{N_1} L_{1,i}(\tau) \mathbb{T}_{1,i} \end{aligned} \tag{19}$$

where $L_{q,i}(\tau)$ are the Lagrange basis polynomials.

*3) Conversion of the State Space Equations:* The differential operation of states can be approximated by the differential operation on the Lagrange basis polynomials, denoted as

$$\dot{\boldsymbol{x}}_q(\tau_{q,k}) = \sum_{i=0}^{N_q} \dot{L}_{q,i}(\tau_{q,k}) \boldsymbol{X}_{q,i} = \sum_{i=0}^{N_q} D_{ki}^q \boldsymbol{X}_{q,i} \tag{20}$$

where, $k = 0, 1, 2, \ldots, N_q$, and $\boldsymbol{D}^q$ is the differentiation matrix with explicit expression [23].

Then Eq. (10) of the pulse phase is forced to satisfy a series of equality constraints at the LGL collocation points,

$$\begin{aligned} &\sum_{i=0}^{N_1} D_{ki}^1 \mathbb{S}_{1,i} = \frac{T_1 - T_0}{2} \mathbb{V}_{1,k} \\ &\sum_{i=0}^{N_1} D_{ki}^1 \mathbb{V}_{1,i} = \frac{T_1 - T_0}{2} \frac{i_g i_0 \eta_T \mathbb{T}_{1,k}/r_w - k_a \mathbb{V}_{1,k}^2 - k_f}{\delta_{i_g} M + i_0 \eta_T \gamma_d k_w i_g^2 \mathbb{T}_{1,k}/r_w}. \end{aligned} \tag{21}$$

Eq. (11) of the glide phase is converted in the same way, i.e.,

$$\begin{aligned} &\sum_{i=0}^{N_2} D_{ki}^2 \mathbb{S}_{2,i} = \frac{T_2 - T_1}{2} \mathbb{V}_{2,k} \\ &\sum_{i=0}^{N_2} D_{ki}^2 \mathbb{V}_{2,i} = \frac{T_2 - T_1}{2} \left( \frac{i_0 i_\mathrm{g}}{\delta_{i_\mathrm{g}} M r_w} \frac{\mathbb{T}_{2,k}}{\eta_T} - \frac{k_a \mathbb{V}_{2,k}^2 + k_f}{\delta_{i_\mathrm{g}} M} \right). \end{aligned} \tag{22}$$

*4) Conversion of the Cost Function:* The integration part of the cost function is calculated by Gaussian-Lobatto quadrature. The performance index in the whole PnG is computed as:

$$J = \frac{(T_1 - T_0) \sum_{i=0}^{N_1} w_{1,i} \mathcal{F}_P + (T_2 - T_1) \sum_{i=0}^{N_2} w_{2,i} \mathcal{F}_G}{2 \mathbb{S}_{2,N_2}} \tag{23}$$

where $w_{1,i}$ and $w_{2,i}$ are the weight coefficients for the Gaussian-Lobatto quadrature, defined as [23]

$$w_{q,i} = \int_{-1}^{1} L_{q,i}(\tau) d\tau = \frac{2}{N_q (N_q + 1) P_{N_q}^2(\tau_{q,i})}. \tag{24}$$

*5) Connection Constraints:* The velocity and distance are continuous between the two phases, therefore connection constraints are added, i.e.,

$$\begin{aligned} \mathbb{S}_{1,N_1} - \mathbb{S}_{2,0} &= 0 \\ \mathbb{V}_{1,N_1} - \mathbb{V}_{2,0} &= 0. \end{aligned} \tag{25}$$

After the above steps, the OCP is converted into a nonlinear programming problem (NLP), described as following:

$$\min\ J = \frac{(T_1 - T_0) \sum_{i=0}^{N_1} w_{1,i} \mathcal{F}_P + (T_2 - T_1) \sum_{i=0}^{N_2} w_{2,i} \mathcal{F}_G}{2 \mathbb{S}_{2,N_2}}.$$

Subject to

$$\sum_{i=0}^{N_q} D_{ki}^{q}\mathbb{S}_{q,i} = \frac{T_q - T_{q-1}}{2}\mathbb{V}_{q,k}$$

$$\sum_{i=0}^{N_1} D_{ki}^{1}\mathbb{V}_{1,i} = \frac{T_1 - T_0}{2}\frac{i_g i_0 \eta_T \mathbb{T}_{1,k}/r_w - k_a\mathbb{V}_{1,k}^2 - k_f}{\delta_{i_g} M + i_0\eta_T\gamma_d k_w i_g^2 \mathbb{T}_{1,k}/r_w}$$

$$\sum_{i=0}^{N_2} D_{ki}^{2}\mathbb{V}_{2,i} = \frac{T_2 - T_1}{2}\left(\frac{i_0 i_g}{\delta_{i_g} M r_w}\frac{\mathbb{T}_{2,k}}{\eta_T} - \frac{k_a\mathbb{V}_{2,k}^2 + k_f}{\delta_{i_g} M}\right)$$

$$\mathbb{T}_{2,k} = \alpha_0 + \alpha_1\left(\frac{\mathbb{W}_{2,k}}{6500}\right) + \alpha_2\left(\frac{\mathbb{W}_{2,k}}{6500}\right)^2$$

$$0 = \mathbb{W}_{q,k} - k_w V_{q,k} i_{gq}$$

$$0 = \frac{\mathbb{S}_{2,N_2}}{T_2} - v_{\mathrm{e}}$$

$$0 = \mathbb{S}_{1,N_1} - S_{2,0}$$

$$\mathbb{V}_{1,N_1} = \mathbb{V}_{2,0} = (1+\beta)v_{\mathrm{e}}$$

$$\mathbb{V}_{1,0} = \mathbb{V}_{2,N_2} = (1-\beta)v_{\mathrm{e}}$$

$$w_{\mathrm{emin}} \le \mathbb{W}_{q,k} \le w_{\mathrm{emax}}$$

$$0 < \mathbb{T}_{q,k} \le T_{\max}(\mathbb{W}_{q,i})$$

$$i_{\mathrm{g}} \in \{i_{\mathrm{g1}}, i_{\mathrm{g2}}, i_{\mathrm{g3}}, i_{\mathrm{g4}}, i_{\mathrm{g5}}\}. \tag{26}$$

where, $\mathbb{W}_{q,i}$ is the discretized engine speed; $k, i = 0, 1, \ldots, N_q$; $q = 1, 2$. In essence, this NLP is a high-dimensional sparse constrained problem. The variables to be optimized include traveling distance $\mathbb{S}_{q,k}$, vehicle speed $\mathbb{V}_{q,k}$, engine torque $T_{q,k}$, gear ratio $i_{\mathrm{g}}$, and time $T_1, T_2$. These variables are continuous except the discrete gear ratio $i_{\mathrm{g}}$. Here the enumeration strategy is adopted to convert the discrete problem into a set of continuous sub-problems, and the NLP is then solved by the sequential quadratic programming algorithm [27].

## IV. Optimization Results and Analysis

In this section, we focus on the optimization results and the fuel saving capacity of the four different PnG strategies.

### A. Optimization Results

We first study a typical driving scenario, i.e., cruising at an average velocity of 70 km/h with 10% velocity fluctuation. The number of collocation points is set to 15 in the pulse phase, and 8 in the glide phase.

For the PnG-G-S strategy, the optimization results show that the optimal performance index is 7.67 L/100 km when gear IV is used, and the optimal velocity and engine operating points (engine speed and torque) are shown in Fig. 3. If using gear II and III, the performance indexes are 13.63 and 8.57 L/100 km, respectively, and the results are also shown in Fig. 3.

In Fig. 3(a), the vehicle first accelerates from 63 km/h to 77 km/h and then coasts down to 63 km/h. Note that the velocity profiles are nearly straight lines because of the small velocity fluctuation and minor change in engine torque, as shown in Fig. 3(c).

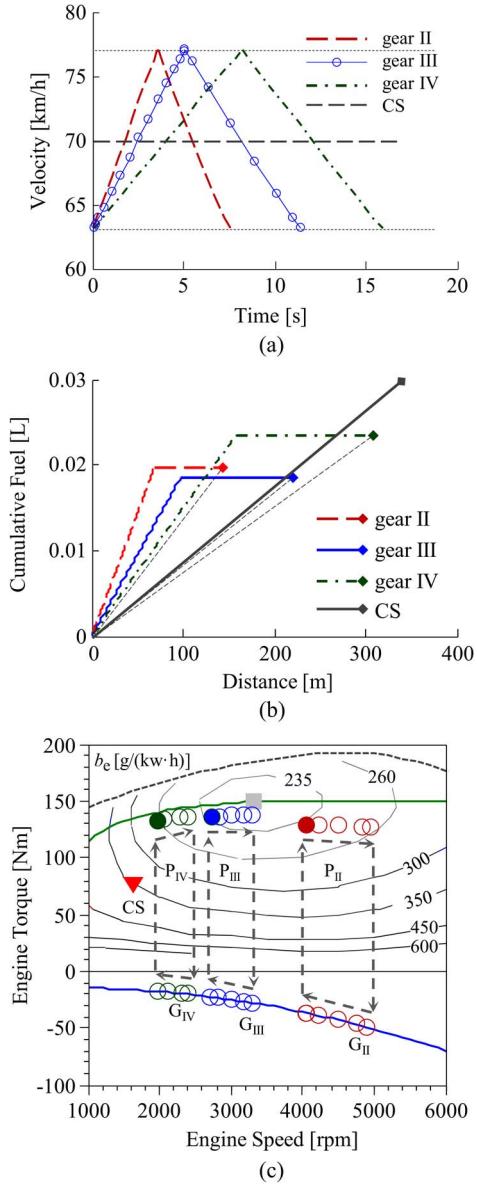


Fig. 3. Optimization results of PnG-G-S using gear II, III, and IV. (a) Velocity profiles; (b) cumulative fuel consumption (c) engine operating points of both the pulse-phase and the glide-phase (where $\mathrm{P}_{\#}$ and $\mathrm{G}_{\#}$ mean pulse and glide with gear #).

Fig. 3(b) shows the cumulative fuel consumption of using different gears. The fuel consumption increases rapidly in the pulse phase, and keeps constant in the glide phase due to the deceleration fuel cut off. The slope of the line between the origin and the endpoint is equal to the performance index $J$, i.e., 13.63, 8.57, and 7.67 L/100 km when using gear II, III, and IV, respectively. The $J$ of CS strategy is 8.83 L/100 km. It is clear that using gear III and IV is more economical than the CS strategy; using gear IV is the best while using gear II is the worst on fuel economy, which can be explained by Fig. 3(c).

Fig. 3(c) shows the distribution of the engine operating points. Using gear II leads to the lowest engine efficiency and highest drag torque, so the fuel economy is the worst. On the other hand, using gear III can have better engine efficiency but higher drag torque than using gear IV, which results in similar fuel economy.

The other three PnG strategies, i.e., PnG-N-O, PnG-N-I, PnG-G-D, are also optimized in this example by the proposed method. The optimal cumulative fuel, vehicle speed, acceleration, and gear position of the four PnG strategies are shown in Fig. 4. We can see that

(1) As shown in Fig. 4(a), the order of fuel economy is PnG-N-O > PnG-N-I > PnG-G-D > PnG-G-S > CS. Their optimal performance indexes are 5.95, 6.70, 7.08, 7.67, and 8.83 L/100 km, respectively. Namely, the fuel-saving rates of PnGs are 32.6%, 24.1%, 19.8%, 13.1% compared to CS, respectively. In the coasting phase, the cumulative fuel of PnG-N-I increases slowly due to the engine idling fuel injection, and the others keep constant because of the shutdown of engine or the function of deceleration fuel cut off.

(2) As mentioned before, the optimal gear of PnG-G-S is gear IV, which is a compromise between the engine efficiency and engine drag torque. While for the other three strategies, the velocity and acceleration trajectories in the accelerating phases are similar, as shown in Fig. 3(b) and (d), and the optimal gear positions are III, which operates the engine more efficiently.

(3) Fig. 4(d) shows that the first three PnG strategies need to periodically switch the gear position. Compared to them, the PnG-G-S has an advantage, i.e., never shift in the entire PnG process, although the fuel saving is the lowest.

### B. Fuel Saving Capacity of the Four PnG Strategies

To analyze the fuel saving of the different PnG strategies, we repeatedly optimize the four PnGs at different average velocity $\bar{v}$ in the range of [30,140] km/h. The fuel consumption of PnG-G-S and the fuel saving rate $\eta_{\mathcal{F}}$ of the four PnGs are shown in Fig. 5. The $\eta_{\mathcal{F}}$ is defined as

$$\eta_{\mathcal{F}} = \frac{J_{\mathrm{CS}} - J_{\mathrm{PnG}}}{J_{\mathrm{CS}}} \times 100\% \tag{27}$$

where $J_{\mathrm{PnG}}$ and $J_{\mathrm{CS}}$ are the performance index of PnG and CS, respectively.

As an example, Fig. 5(a) shows the fuel consumption (L/100 km) of PnG-G-S and CS at different average cruising speed using different gears. In Fig. 5(a), the red envelope of $P_{\mathrm{III}}$, $P_{\mathrm{IV}}$, and $P_{\mathrm{V}}$ stands for the optimal fuel consumption of PnG-G-S. PnG-G-S has better fuel economy than CS in the speed range [30, 120] km/h. The fuel saving rate of the four strategies compared to CS are shown in Fig. 5(b), as well as the optimal gears used in the pulse phase.

In Fig. 5(b), we can see that PnG strategies can only save fuel in the range of [30, 120] km/h for the studied vehicle. The highest fuel saving rate is 45% at 46 km/h. Note that the fuel saving capacity is the theoretical optimal results, which ignores the negative impact of frequent engine start-stop and gear shifting.

We emphasize that higher fuel saving capacity is not the only factor to be considered for implementation. The pros and cons of the four different PnG strategies are summarized in Table II.

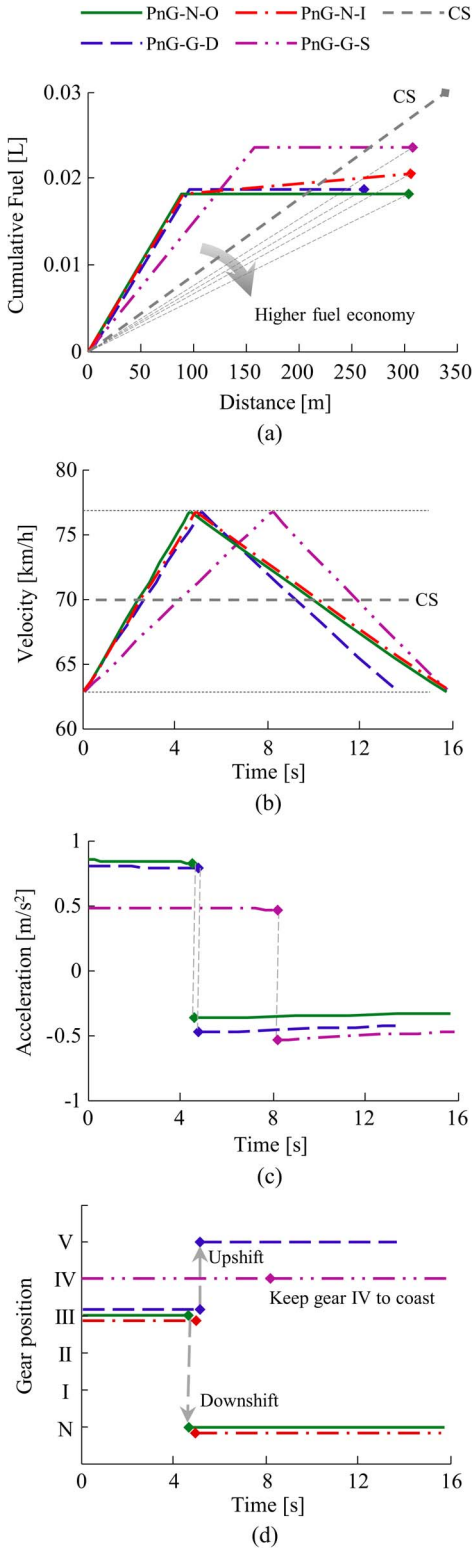


Fig. 4. Optimization results of the four PnG strategies ($\bar{v}$ is 70 km/h). (a) Cumulative fuel consumption; (b) optimal velocity trajectory; (c) optimal acceleration trajectory; (d) optimal gear position.

## V. Mechanism of the Pulse-and-Glide Operation

In this section, we focus on the following questions:

(Q1) Why can the PnG operation save fuel compared to CS;

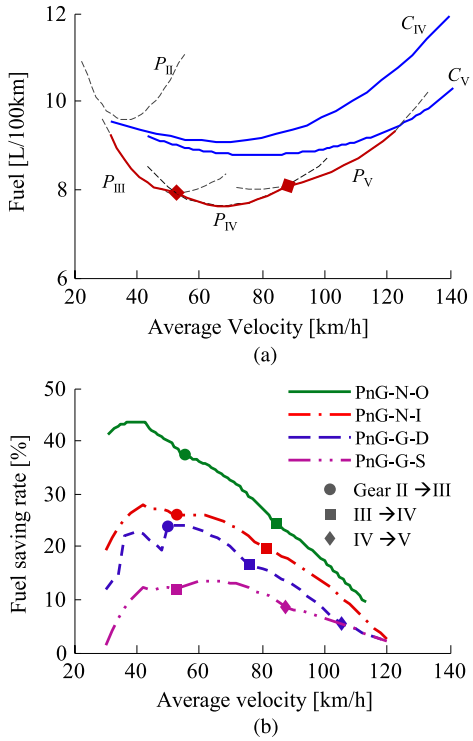


Fig. 5. Optimal fuel saving capacity of the four PnG strategies. (a) Fuel consumption of PnG-G-S at different $\bar{v}$ ($P_X$: PnG with gear X, $C_X$: CS with gear X); (b) Optimal fuel saving rates.

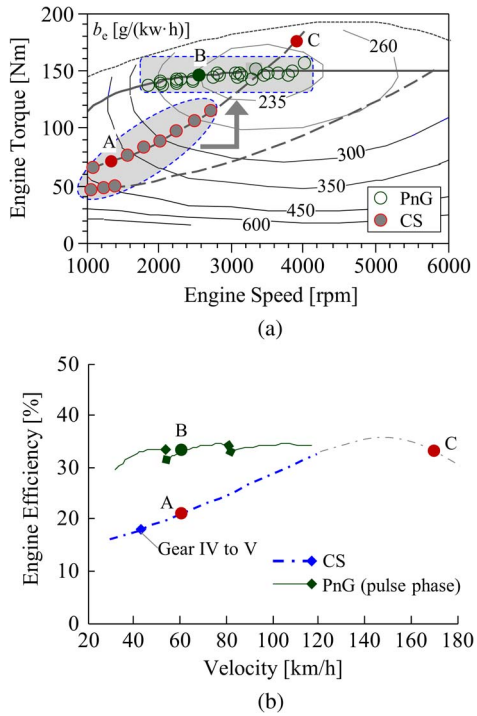


Fig. 6. Comparison between the CS strategy and the PnG-N-I strategy. (a) Distribution of the engine operating points for cruising speed between [30, 120] km/h; (b) improvement of engine efficiency using PnG strategy.

TABLE II
PROS AND CONS OF THE FOUR PNG STRATEGIES

| Strategy | Pros (F: fuel) | Cons |
|---|---|---|
| PnG-N-O | F: ★★★★ | Frequent engine start/stop<br>Frequent gear shift |
| PnG-N-I | F: ★★★ | Frequent gear shift<br>Prolonged idling |
| PnG-G-D | F: ★★ | Frequent gear shift |
| PnG-G-S | F: ★<br>No gear shifting | |
| CS | Constant speed | Relatively poor fuel economy |

(Q2) Why is the fuel saving capacity in the order of PnG-N-O > PnG-N-I > PnG-G-D > PnG-G-S for the studied vehicle;

(Q3) What is the relationship between gear selection and fuel saving.

For Q1, due to the performance consideration such as maximum grade and maximum speed, vehicles are always equipped with an engine whose maximum power is much higher than the power needed for cruising. For the studied engine, the maximum power is greater than 100 kW and the power at the sweet spot is 52 kW, while the required cruising power is only 10.3 kW at 60 km/h. So the engine always operates at inefficient area using the CS strategy, as shown in Fig. 6. The point $A$ indicates cruising at 60 km/h by CS, the engine efficiency is only 21%. The low efficiency directly leads to the low fuel economy of CS.

The PnG operation can increase the engine efficiency significantly. In the pulse phase, PnG usually uses a lower gear than CS to ensure the engine speed in the interval of [2000, 4000] rpm and keeps the engine operating efficiently (e.g., at point $B$). The distribution of engine operating points of PnG-N-I is shown in Fig. 6(a). When cruising at 60 km/h, the PnG strategy can increase the engine efficiency from 21% (point A) to 33% (point $B$), as shown in Fig. 6(b). Although the engine output power and fuel injection rate are quite high in the pulse phase, the engine can efficiently convert the chemical energy into the mechanical energy, which is stored in the form of kinetic energy, and then dissipated in the glide phase. Overall, in the PnG strategy the engine is "operating efficiently but intermittently," which leads to better fuel economy than "operating steadily but less-efficiently" in the CS strategy. However, the engine drag torque, idling fuel, and dynamic torque loss will make the fuel saving rate lower than the ideal.

Fig. 7 is designed as the key figure to understand the fuel saving mechanisms and to answer the three questions. The positive vertical axis represents the fuel injection rate and the negative vertical axis represents the average cruising velocity. The horizontal axis represents the drive power (positive) and drag power (negative). We made the following simplification:

(a) Since the optimal engine operating points are near the line EL in the pulse phase, as shown in Fig. 6(a), the engine is approximated to always operate on line EL;

(b) At a certain average speed, the engine torque trajectory is concentrated to a single point, e.g., at point $P_{III}$ (in Fig. 7) to accelerate the vehicle.

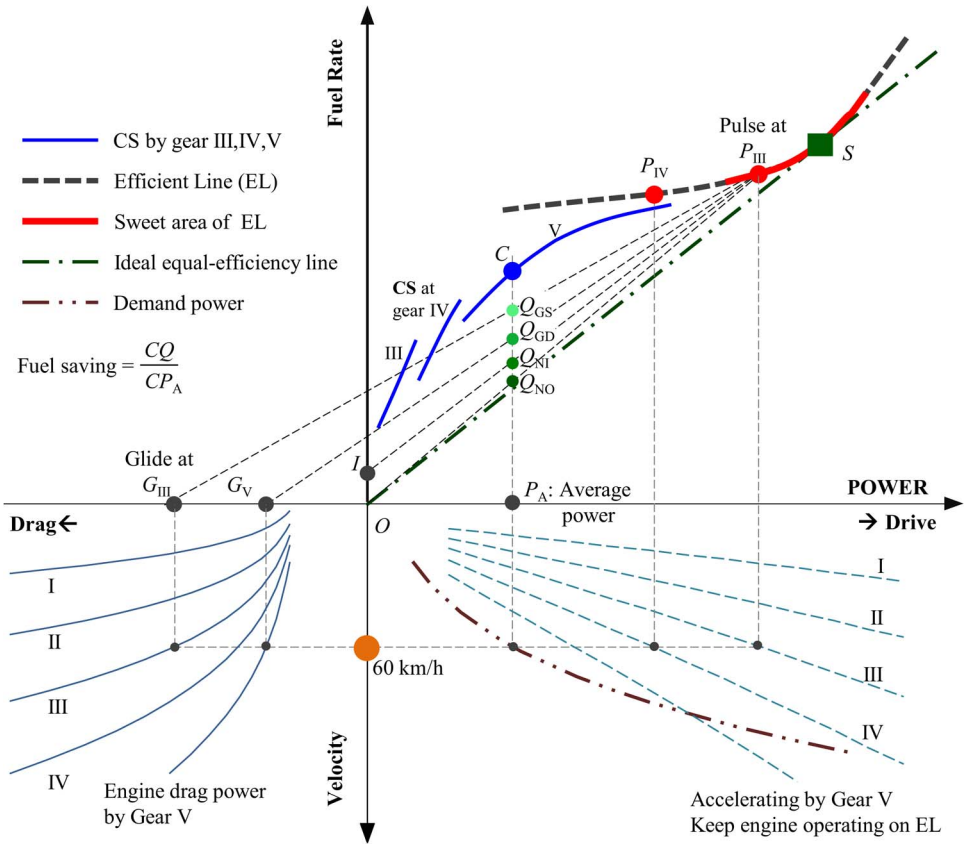


Fig. 7. Mechanism of PnG type cruising strategy.

As an example, when cruising at 60 km/h, the average demanded power, shown as point $P_{\mathrm{A}}$, is decided by the double dot dash in the fourth quadrant. If the CS strategy is used, the engine keeps operating at point $C$ using gear V. If using the PnG strategy:

- In the pulse phase, since the engine operates on EL, the engine output power using each of the five gears is determined by the five dotted lines in the fourth quadrant. So the engine operates at point $P_{\mathrm{III}}$ if using gear III, or at point $P_{\mathrm{IV}}$ if using gear IV.
- In the glide phase, when coasting with transmission in neutral and engine shutting down/idling, the engine operates on points $O/I$, resulting PnG-N-O/PnG-N-I; when coasting with transmission in gear, the engine drag power is determined by the five lines in the third quadrant. If the gears for coasting and accelerating are the same, we get PnG-G-S; otherwise we get PnG-G-D.
- Since the average demanded power of CS and PnG strategies are the same, the points $Q_{\mathrm{NO}}$, $Q_{\mathrm{NI}}$, $Q_{\mathrm{GD}}$, and $Q_{\mathrm{GS}}$ are the average points of PnG-N-O, PnG-N-I, PnG-G-D, and PnG-G-S strategies, respectively. The line $CP_{\mathrm{A}}$ stands for the fuel consumption of CS, $Q_{\#}P_{\mathrm{A}}$ stands for the fuel consumption of PnGs, and $CQ_{\#}$ indicates the saved fuel.

Due to the strong nonlinearity of the engine, the fuel injection rate of CS appears like a "discontinuous concave function" as shown in Fig. 7. In PnGs, the engine operates between the high-efficiency area (near point $S$) and the point $I$ (or $O, G$), then the average fuel rates are much lower than that of CS. This is another way to show the mechanism of fuel saving for PnG strategies.

For Q2, since the point $O$ is always lower than point $I$, the point $Q_{\mathrm{NO}}$ is always lower than $Q_{\mathrm{NI}}$. Namely, PnG-N-O always has better fuel economy than PnG-N-I. Since a higher gear $(G_{\mathrm{V}})$ always leads to a lower drag torque, PnG-G-D always has better fuel economy than PnG-G-S. However, we cannot tell PnG-N-I or PnG-G-D is better because the answer depends on the relative position of points $I$ and $G_{\mathrm{V}}$. For the studied vehicle, point $I$ (idling fuel) has lower negative effect than point $G_{\mathrm{V}}$ (engine drag torque), so PnG-N-I has better fuel economy. Here $OS$ is the fuel rate limit of PnG strategies because no point can exist below this line.

For Q3, we can qualitatively conclude from Fig. 7:

(a) The *optimal* gear not only depends on the engine efficiency, but also depends on the engine states in the coasting phase (points $O$, $I$, and $G$).
(b) For PnG-G-S, the optimal gear is the result of compromising between the engine efficiency and drag torque.
(c) For the other PnGs, in the pulse phase, the optimal gear is the one leading to maximum engine efficiency. In the glide phase, PnG-N-O and PnG-N-I always use the neutral gear, and PnG-G-D always select the highest admissible gear to minimize engine drag.

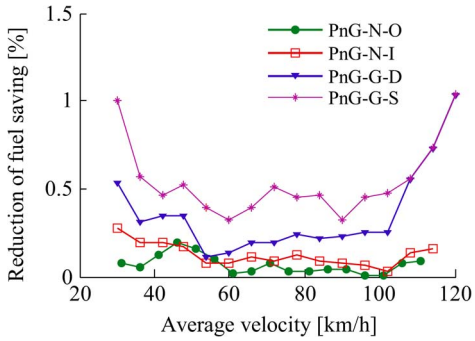


Fig. 8. Reduction of fuel saving rate when taking the simplification on engine operation.

## VI. Implementable Strategy

The optimal control solution can be approximated by simple rules while making it easier for real-time implementation.

In Fig. 6(a), we see that the optimal engine operating points are near the line EL in the pulse phase. Therefore, here we simplify the control strategy of engine for all of the four PnG strategies as "always keep the engine operating on the efficient line EL." Under this simplification, the difference of fuel saving rate between the simplified strategy and the optimum (in Fig. 5(b)) is shown in Fig. 8, where the fuel saving rates of the four PnGs decrease less than one percentage point.

The optimal gear positions for the four PnGs obtained by the massive optimization results are shown in Fig. 9(b). We simplify the control strategy of transmission based on Fig. 7, i.e., "always select the gear that enables highest engine efficiency." Namely, we should keep the engine operating on the line EL, and then select the gear to maximize the engine efficiency. The optimal gear is defined as

$$i_{\mathrm{g}}^{*} = \arg\max_{i_{\mathrm{g}}} \{\eta_{\mathrm{e}}(w_{\mathrm{e}}, T_{\mathrm{e}}) | w_{\mathrm{e}} = k_w \bar{v} i_{\mathrm{g}}, (w_{\mathrm{e}}, T_{\mathrm{e}}) \in EL\} \quad (28)$$

where $\eta_{\mathrm{e}}(w_{\mathrm{e}}, T_{\mathrm{e}})$ is the engine efficiency.

For the studied vehicle, if keeping the engine on line EL, the engine efficiency of using different gears is shown in Fig. 9(a). The intersections are the simplified gear switching points. The resulting gear selecting map is shown in Fig. 9(b). Taking the simplification on engine and transmission, the decline of fuel saving rate is shown in Fig. 9(c). We can see that the fuel saving rate decrease less than 4 percentage points for PnG-N-O, PnG-N-I, and PnG-G-D. However, this simplification is not applicable for PnG-G-S, whose optimal gear is highly related to the engine drag.

These practical rules mean that for a new vehicle, if we know the efficient line EL (its speeds, torque, and fuel rate) of the engine and the gear ratios of the transmission, we can quickly and easily design a near-optimal control rule for PnG operations without sacrificing fuel saving too much.

## VI. Conclusion

In this paper, we quantitatively studied the PnG-type cruising strategy for road vehicles with a step-gear transmission. The major findings include the following:

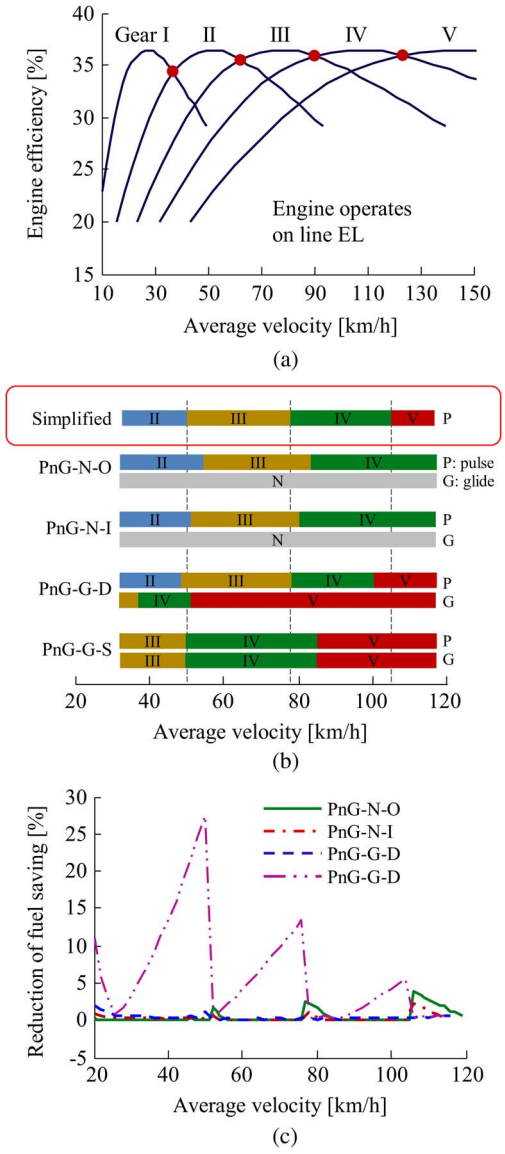


Fig. 9. Practical control rule of transmission gear position and its performance. (a) The engine efficiency on the line EL using the five gears; (b) the optimal gear for both the pulse and glide phases; (c) the reduction in fuel saving rate of the simplified control strategy.

(1) For vehicles with discrete gear ratios, the accurate control on engine and transmission for PnG strategy can be obtained by a discontinuous nonlinear mixed-integer OCP. The proposed multi-phase knotting technique and Legendre pseudospectral discretization converts the problem into a nonlinear programming problem for numerical calculations.

(2) The PnG strategies achieve better fuel economy than CS strategy when average cruising speed $\in [30\ 120]$ km/h for the studied vehicle, and the fuel saving capacities of the four PnGs with different coasting operations are ordered by PnG-N-O > PnG-N-I > PnG-G-D > PnG-G-S. As the speed increases, the fuel saving rate gradually reduces. The pros and cons of the four PnGs are summarized in Table II.

(3) The efficiency of an internal combustion engine is pretty low at light load, while cruising at medium speed

often falls into this low-efficiency area. In PnG, the engine intermittently operates at the high-efficiency area with a high power output, which avoids the inefficient operation.

(4) To be practical, the engine can approximately operate on the economical line EL in the pulse phase, and the optimal gear can be selected as the one that maximizes the engine efficiency for PnGs besides PnG-G-S.

The PnG-type cruising strategy needs to accurately and periodically control the engine and transmission, which makes it difficult to execute by ordinary drivers. However, it is possible to apply PnG-type strategy in the future, e.g., on adaptive cruise control system. We should emphasize that PnG operation may impact the powertrain lifespan, safety, and ride comfort. To avoid such fluctuation on vehicle speed, using a battery, flywheel, or super capacitor to absorb and dissipate the kinetic energy maybe better alternatives.

## ACKNOWLEDGMENT

The first two authors, S. Xu and S. Eben Li, have contributed equally to this work.

## REFERENCES

[1] J. N. Barkenbus, "Eco-driving: An overlooked climate change initiative," *Energy Policy*, vol. 38, no. 2, pp. 762–769, Feb. 2010.
[2] E. W. Martin and S. A. Shaheen, "Greenhouse gas emission impacts of carsharing in North America," *IEEE Trans. Intell. Transp. Syst.*, vol. 12, no. 4, pp. 1074–1086, Dec. 2011.
[3] M. Barth and K. Boriboonsomsin, "Energy and emissions impacts of a freeway-based dynamic eco-driving system," *Transp. Res. Part D, Transp. Environ.*, vol. 14, no. 6, pp. 400–410, Aug. 2009.
[4] E. Ericsson, "Independent driving pattern factors and their influence on fuel-use and exhaust emission factors," *Transp. Res. Part D, Transp. Environ.*, vol. 6, no. 5, pp. 325–345, Sep. 2001.
[5] K. Boriboonsomsin, M. Barth, and A. Vu, "Evaluation of driving behavior and attitude towards eco-driving: A Southern California limited case study," presented at the 90th Annual Meeting of the Transportation Research Board, Washington, DC, USA, 2011.
[6] A. A. Malikopoulos and J. P. Aguilar, "An optimization framework for driver feedback systems," *IEEE Trans. Intell. Transp. Syst.*, vol. 14, no. 2, pp. 955–964, Jun. 2013.
[7] A. Riener, "Subliminal persuasion and its potential for driver behavior adaptation," *IEEE Trans. Intell. Transp. Syst.*, vol. 13, no. 1, pp. 71–80, Mar. 2012.
[8] A. Riener and J. Reder, "Collective data sharing to improve on driving efficiency and safety," in *Proc. 6th Int. Conf. Autom. User Interfaces Interactive Veh. Appl.*, 2014, pp. 1–6.
[9] H. Y. Tong, W. T. Hung, and C. S. Cheung, "On-road motor vehicle emissions and fuel consumption in urban driving conditions," *J. Air Waste Manage. Assoc.*, vol. 50, no. 4, pp. 543–554, Apr. 2000.
[10] M. Fu *et al.*, "$NO_x$ emissions from Euro IV busses with SCR systems associated with urban, suburban and freeway driving patterns," *Sci. Total Environ.*, vol. 452, pp. 222–226, May 2013.
[11] A. E. Atabani, I. A. Badruddin, S. Mekhilef, and A. S. Silitonga, "A review on global fuel economy standards, labels and technologies in the transportation sector," *Renew. Sustain. Energy Rev.*, vol. 15, no. 9, pp. 4586–4610, Dec. 2011.
[12] J. Lee, D. J. Nelson, and H. Lohse-Busch, "Vehicle inertia impact on fuel consumption of conventional and hybrid electric vehicles using acceleration and coast driving strategy," SAE, Warrendale, PA, USA, SAE Techn. Paper, No. 2009-01-1322, 2009.
[13] S. E. Li and H. Peng, "Strategies to minimize the fuel consumption of passenger cars during car-following scenarios," *Proc. IEEE Inst. Mech. Eng., Part D, J. Automobile Eng.*, vol. 226, no. 3, pp. 419–429, 2012.
[14] S. E. Li *et al.*, "Minimum fuel control strategy in automated car-following scenarios," *IEEE Trans. Veh. Technol.*, vol. 61, no. 3, pp. 998–1007, Mar. 2012.
[15] S. E. Li, S. Xu, G. Li, and B. Cheng, "Periodic cruising control of passenger cars for optimized fuel consumption," in *Proc. IEEE Intell. Veh. Symp.*, Dearborn, MI, USA, Jun. 8–11, 2014, pp. 1097–1102.
[16] C. G. Cassandras, D. L. Pepyne, and Y. Wardi, "Optimal control of a class of hybrid systems," *IEEE Trans. Autom. Control*, vol. 46, no. 3, pp. 398–415, Mar. 2001.
[17] M. S. Branicky, V. S. Borkar, and S. K. Mitter, "A unified framework for hybrid control: Model and optimal control theory," *IEEE Trans. Autom. Control*, vol. 43, no. 1, pp. 31–45, Jan. 1998.
[18] M. Gerdts, "Solving mixed-integer optimal control problems by branch & bound: A case study from automobile test-driving with gear shift," *Opt. Control Appl. Methods*, vol. 26, no. 1, pp. 1–18, 2005.
[19] S. Sager, "Numerical methods for mixed-integer optimal control problems," Ph.D. dissertation, University Interdisciplinary Center Sci. Comput., Heidelberg, Germany, 2005.
[20] M. Hu, "Study on energy management strategy for mild hybrid electrical vehicle with CVT," Ph.D. dissertation, Dept. Mech. Eng. Chongqing Univ., Chongqing, China, 2007.
[21] R. W. Knoebel, K. Kar, and R. Goode, "Deceleration Fuel Cutoff Control Systems and Methods," U.S. Patent Appl. 13/358,810[P], Jan. 26, 2012.
[22] I. M. Ross and F. Fahroo, "Pseudospectral knotting methods for solving non-smooth optimal control problems," *J. Guid., Control, Dyn.*, vol. 27, no. 3, pp. 397–405, May/Jun. 2004.
[23] G. Elnagar, M. A. Kazemi, and M. Razzaghi, "The pseudospectral Legendre method for discretizing optimal control problems," *IEEE Trans. Autom. Control*, vol. 40, no. 10, pp. 1793–1796, Oct. 1995.
[24] S. Xu, S. E. Li, K. Deng, S. Li, and B. Cheng, "A unified pseudospectral computational framework for optimal control of road vehicles," *IEEE/ASME Trans. Mechatron.*, vol. 20, no. 4, pp. 1499–1510, Aug. 2015.
[25] I. M. Ross and M. Karpenko, "A review of pseudospectral optimal control: From theory to flight," *Annu. Rev. Control*, vol. 36, no. 2, pp. 182–197, Dec. 2012.
[26] D. Garg *et al.*, "A unified framework for the numerical solution of optimal control problems using pseudospectral methods," *Automatica*, vol. 46, no. 11, pp. 1843–1851, Nov. 2010.
[27] P. E. Gill, W. Murray, and M. A. Saunders, "SNOPT: An SQP algorithm for large-scale constrained optimization," *SIAM rev.*, vol. 47, no. 1, pp. 99–131, 2005.

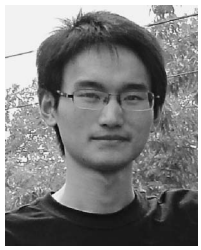

**Shaobing Xu** received the B.S. degree in automotive engineering from China Agricultural University, Beijing, China, in 2011. He is currently working toward the Ph.D. degree in automotive engineering with State Key Laboratory of Automotive Safety and Energy, Department of Automotive Engineering, School of Mechanical Engineering, Tsinghua University, Beijing, China.

His research interests include optimal control theory and vehicle dynamics control. Mr. Xu was a recipient of the National Scholarship, the President Scholarship, the First Prize of the Chinese 4th Mechanical Design Contest, and the First Prize of the 19th Advanced Mathematical Contest.

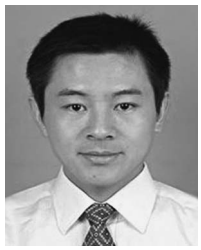

**Shengbo Eben Li** (M'11) received the M.S. and Ph.D. degrees in automotive engineering from Tsinghua University, Beijing, China, in 2006 and 2009, respectively.

In 2007, he was a Visiting Researcher with Stanford University, Stanford, CA, USA, and from 2009 to 2011, he was a Postdoctoral Research Fellow with University of Michigan, Ann Arbor, MI, USA. He is currently an Associate Professor with State Key Laboratory of Automotive Safety and Energy, Department of Automotive Engineering, School of Mechanical Engineering, Tsinghua University. His active research interests include autonomous vehicle control, optimal and predictive control, driver assistance systems, and lithium ion battery management. Dr. Li was the recipient of the Award for Science and Technology of China ITS Association in 2012, the Award for Technological Invention in the Ministry of Education in 2012, the National Award for Technological Invention in China in 2013, and the Honored Funding for Beijing Excellent Youth Researcher in 2013.

**Xiaowu Zhang** received the B.S. degree in mechanical engineering from Beihang University, Beijing, China, in 2010 and the M.S. degree in mechanical engineering from University of Michigan, Ann Arbor, MI, USA, in 2012. He is currently working toward the Ph.D. degree in mechanical engineering with the Department of Mechanical Engineering, College of Engineering, University of Michigan.

His research interests include optimal control, sizing and design of clean energy systems, and configuration design and control of split hybrid vehicles.

**Bo Cheng** received the B.S. and M.S. degrees in automotive engineering from Tsinghua University, Beijing, China, in 1985 and 1988, respectively, and the Ph.D. degree in mechanical engineering from Tokyo University, Tokyo, Japan, in 1998.

He is a Professor with Tsinghua University, where he is also the Dean of the Suzhou Automotive Research Institute. His active research interests include autonomous vehicles, driver assistance systems, active safety, vehicular ergonomics, etc. Dr. Cheng works as the Chair of the Academic Board of SAE Beijing, as a member of the Council of the Chinese Ergonomics Society, and as a Committee Member of the National 863 Plan.

**Huei Peng** received the Ph.D. degree in mechanical engineering from the University of California Berkeley, Berkeley, CA, USA, in 1992.

He is currently a Professor with the Department of Mechanical Engineering, College of Engineering, University of Michigan, Ann Arbor, MI, USA. He is also a Changjiang Scholar with State Key Laboratory of Automotive Safety and Energy, Department of Automotive Engineering, School of Mechanical Engineering, Tsinghua University, Beijing, China. His research focuses include the design and control of electrified vehicles, and connected/automated vehicles. His research interests include adaptive control and optimal control, with emphasis on their applications to vehicular and transportation systems. Dr. Peng is a fellow of SAE and ASME.